Closing the circadian negative feedback loop:

FRQ-dependent clearance of WC-1 from the nucleus

Supplementary Material

Christian I. Hong[1], Peter Ruoff[2], Jennifer J. Loros[1,3], and Jay C. Dunlap[1]

[1]Dartmouth Medical School

Department of Genetics

HB 7400

Hanover, NH 03755

[2]University of Stavanger

Centre for Organelle Research

Faculty of Science and Technology

N-4036

Stavanger, Norway

[3]Dartmouth Medical School

Department of Biochemistry

HB 7400

Hanover, NH 03755

Corresponding Author: Jay.C.Dunlap@Dartmouth.edu

The Model

The two models shown in Fig. 5 are slight variations of a model proposed and discussed previously (Hong et al. 2008). We here summarize the components of the models and their rate equations.

Steps 1-6 represent the expression of *frq*, including transcription (step 1), translation (step 2) and translocation of FRQ protein into the nucleus (step 3), the degradation of *frq* mRNA (step 4), as well as degradation of cytosolic and nuclear FRQ (steps 5-6). Because there is much less nuclear FRQ than cytoplasmic FRQ, and because the degradation rate constant of nuclear FRQ (k_6) is significantly lower than the cytosolic FRQ degradation rate constant (k_5), in the model the degradation of total FRQ is mostly determined by the cytosolic FRQ degradation. The cytosolic FRQ degradation rate constants are in good agreement with experimental estimates of total FRQ degradation (Table 1, Ref. 29). The results from the model remain similar even when k_5 and k_6 values are set equal to the experimental FRQ degradation rate constants but with slightly shorter periods and reduced amounts of FRQ. Steps 7-12 represent the expression of *wc-1* and nuclear localization of WC-1 with degradation reactions (steps 10-12). WC-2 is present in excess over WC-1 and the concentration of WC-2 does not change during the circadian cycle (Cheng et al. 2001; Denault et al. 2001). Therefore, we consider WC-2 as a constant and have not included WC-2 in the model. In addition, the WCC complex is represented by WC-1_n. Step 8 describes the FRQ promoted accumulation of WC-1. The step with rate constant k_{02} represents a minor contribution to WC-1_c synthesis in the absence of FRQ (Lee et al. 2000; Cheng et al. 2001; Schafmeier et al. 2006). Steps 13-15 represent the inactivation of WC-1_n by binding to FRQ_n with a 1:1 stoichiometry.

While we previously only considered a degradation of the WC-1_n:FRQ_n complex (Hong et al. 2008), we now include the export of the complex in the cytoplasm, where degradation or inactivation of the complex occurs (steps 16-18).

Step 19 represents the binding of WC-1_n at the *frq* promoter. The *frq* promoter contains two light responsive elements (LREs), where the distal element ("the clock (C)-box") (Froehlich et al. 2003) appears necessary for rhythmicity (Froehlich et al. 2002). Each LRE contains two GATN sequence repeats each probably capable of binding the Zn-finger domain from either WC-1 or WC-2. In its present form, the model suggests that at least two WC-1_n molecules need to bind to the promoter (C-box), because a reaction order lower than 2 (with respect to [WC-1_n], see Eq. 1a) does not generate oscillations. With an increasing reaction order/Hill coefficient ≥ 2 oscillations are more easily generated with a larger oscillatory domain, which was also observed in other studies; see for example Ref. (Yu et al. 2007). The binding of WC-1_n to the *frq* promoter is described as a rapid equilibrium with dissociation constant *K* leading to Eqs. 1a and 2a in the *frq* transcription rate (Hong et al. 2008).

The rate equations for the model in Fig. 5A model are:

$$\frac{d[\,frq\ mRNA]}{dt} = k_1 \frac{[WC-1_n]^2}{K+[WC-1_n]^2} - k_4[\,frq\ mRNA] + k_{01} \tag{1a}$$

$$\frac{d[FRQ_c]}{dt} = k_2[\,frq\ mRNA] - (k_3 + k_5)[FRQ_c] \tag{1b}$$

$$\frac{d[FRQ_n]}{dt} = k_3[FRQ_c] + k_{14}[FRQ_n : WC-1_n] - [FRQ_n](k_6 + k_{13}[WC-1_n]) \quad (1c)$$

$$\frac{d[wc-1\ \ mRNA]}{dt} = k_7 - k_{10}[wc-1\ \ mRNA] \quad (1d)$$

$$\frac{d[WC-1_c]}{dt} = \frac{k_8[FRQ_c][wc-1\ \ mRNA]}{K_2 + [FRQ_c]} - (k_9 + k_{11})[WC-1_c] + k_{02}[wc-1\ \ mRNA] \quad (1e)$$

$$\frac{d[WC-1_n]}{dt} = k_9[WC-1_c] - [WC-1_n](k_{12} + k_{13}[FRQ_n]) + k_{14}[FRQ_n : WC-1_n] \quad (1f)$$

$$\frac{d[FRQ_n : WC-1_n]}{dt} = k_{13}[FRQ_n][WC-1_n] - (k_{14} + k_{15} + k_{16})[FRQ_n : WC-1_n] + k_{17}[FRQ_c : WC-1_c] \quad (1g)$$

$$\frac{d[FRQ_c : WC-1_c]}{dt} = k_{16}[FRQ_n][WC-1_n] - (k_{17} + k_{18})[FRQ_c : WC-1_c] \quad (1h)$$

Concentrations in arbitrary units (a.u.) reflect the number of molecules/moles per cell/septum department. Table 1 shows the rate constants used in the results shown below. Experimentally determined rate constants are indicated in Table 1 by an asterisk and the corresponding references. The other rate constants have been chosen to fit the model to experimental observations such as phase relationships between different components and various mutant behaviors (Hong et al. 2008).

Fig. 5B shows an alternative version of closing the negative feedback loop, where FRQ is recycled, i.e., the FRQ_n:$WC\text{-}1_n$ complex is translocated into the cytosol where inactive WC-1 is formed, while FRQ remains intact and active. The rate equations in this case are:

$$\frac{d[\,frq\ mRNA]}{dt} = k_1 \frac{[WC-1_n]^2}{K+[WC-1_n]^2} - k_4[\,frq\ mRNA] + k_{01} \tag{2a}$$

$$\frac{d[FRQ_c]}{dt} = k_2[\,frq\ mRNA] - (k_3+k_5)[FRQ_c] + k_{18}[FRQ_c : WC-1_c] \tag{2b}$$

$$\frac{d[FRQ_n]}{dt} = k_3[FRQ_c] + k_{14}[FRQ_n : WC-1_n] - [FRQ_n](k_6 + k_{13}[WC-1_n]) \tag{2c}$$

$$\frac{d[wc-1\ \ mRNA]}{dt} = k_7 - k_{10}[wc-1\ \ mRNA] \tag{2d}$$

$$\frac{d[WC-1_c]}{dt} = \frac{k_8[FRQ_c][wc-1\ \ mRNA]}{K_2+[FRQ_c]} - (k_9+k_{11})[WC-1_c] + k_{02}[wc-1\ \ mRNA] \tag{2e}$$

$$\frac{d[WC-1_n]}{dt} = k_9[WC-1_c] - [WC-1_n](k_{12}+k_{13}[FRQ_n]) + k_{14}[FRQ_n : WC-1_n] \tag{2f}$$

$$\frac{d[FRQ_n : WC-1_n]}{dt} = k_{13}[FRQ_n][WC-1_n] - (k_{14}+k_{15}+k_{16})[FRQ_n : WC-1_n] + k_{17}[FRQ_c : WC-1_c] \tag{2g}$$

$$\frac{d[FRQ_c : WC-1_c]}{dt} = k_{16}[FRQ_n][WC-1_n] - (k_{17} + k_{18})[FRQ_c : WC-1_c] \quad \text{(2h)}$$

Influence of nuclear FRQ:WC-1 Complex Stability, its Cytosolic Shuttling and the FRQ:WC-1 Complex Turnover on Oscillations

In order to estimate the relative contributions of the FRQ:WC-1 complex stability, and its FRQ-dependent clearance out of the nucleus (either by degradation or cytosolic shuttling), we first consider the somewhat artifical situation that no degradation or shuttling into the cytoplasm of nuclear FRQ:WC-1 can occur. This is simulated by setting rate constants k_{15} and k_{16} to zero. Using the wild-type rate constants of Table 1 (Hong et al. 2008), Fig. S1A shows that damped oscillations in the production rate of total FRQ are observed, while total WC-1 is not oscillatory but increases with constant rate. As previously shown (Hong et al. 2008), stable oscillations in FRQ and WC-1 can be observed when the nuclear FRQ:WC-1 complex is sufficiently rapid degraded.

Stable oscillations in the rate of FRQ production are also observed when the stability constant (i.e., the ratio k_{14}/k_{13}) of the nuclear FRQ:WC-1 complex is made sufficiently large. In Fig. S1B rate constant k_{14} is increased by 3 orders of magnitude to 5×10^4 a.u. h^{-1}. Interestingly, stable oscillations in the rate of total FRQ production are now observed, while total WC-1 is not oscillatory. This clearly shows that stable oscillations in the rate of total FRQ production may be observed without any removal of the FRQ:WC-1 complex out of the nucleus. However, in order to obtain the observed oscillatory phenotype, that is, oscillations in both FRQ and WC-1 around a quasi-constant mean, the nuclear FRQ:WC-1 complex needs to be cleared from the nucleus, either by degradation (Hong et al. 2008) or by shuttling into the cytoplasm.

Fig. S1C shows that stable oscillations in total FRQ and WC-1 occur when nuclear FRQ:WC-1 is translocated into the cytosol and there degraded (Fig. 5A), while nuclear FRQ:WC-1 is now not considered to be degraded in the nucleus (k_{15}=0).

It was recently suggested that nuclear FRQ may promote, in a 'catalyst-like' manner, the deactivation of WC-1/WCC (Schafmeier et al. 2005; Schafmeier et al. 2006). Fig. 5B shows a mechanism, where nuclear FRQ:WC-1 is shuttling between cytoplasm and nucleus, but in the cytoplasm the complex dissociates into an inactive WC-1 form while FRQ is recycled and remains active. The corresponding calculations are shown in Fig. S1D. While the amplitude of total FRQ and the period of oscillations in Fig. S1D are slightly larger than in Fig. S1C, the relative phase differences between total WC-1 and total FRQ are practically identical and similar to previous calculations and experimental observations (Hong et al. 2008).

It is also interesting to note that the period length of the oscillations shown in Fig. S1 B, C, and D are not affected by the rate constants k_{16}, k_{17} or k_{18}, indicating that the core mechanism behind the oscillations is the timed interaction between nuclear WC-1 and the *frq*-promoter leading to the production of cytosolic FRQ and the relative tight binding between FRQ and WC-1 in the nucleus. However, in order to account for the observed phenotype of the oscillations and to avoid an overall buildup of FRQ and WC-1 in the nucleus, nuclear FRQ:WC-1 must be cleared either by degradation in the nucleus (Hong et al. 2008) or by shuttling mechanisms as the two shown in Fig. 5.

Fig. S2 shows the oscillation profiles for nuclear FRQ, nuclear WC-1, and the nuclear FRQ:WC-1 complex for the two shuttling mechanisms shown in Fig. 5. As for the nuclear FRQ:WC-1 degradation mechanism (Hong et al. 2008), nuclear FRQ and

WC-1 oscillate in anti-phase and with clear oscillations of the nuclear FRQ:WC-1 complex (Fig. S2) and the cytosolic complex (data not shown).

Computational methods

The differential equations were solved numerically and analyzed by using the FORTRAN subroutine LSODE (Radhakrishnan and Hindmarsh 1993) and XPPAUT (Ermentrout 2002). Ode-files, FORTRAN codes, and MATLAB versions of the two models are available.

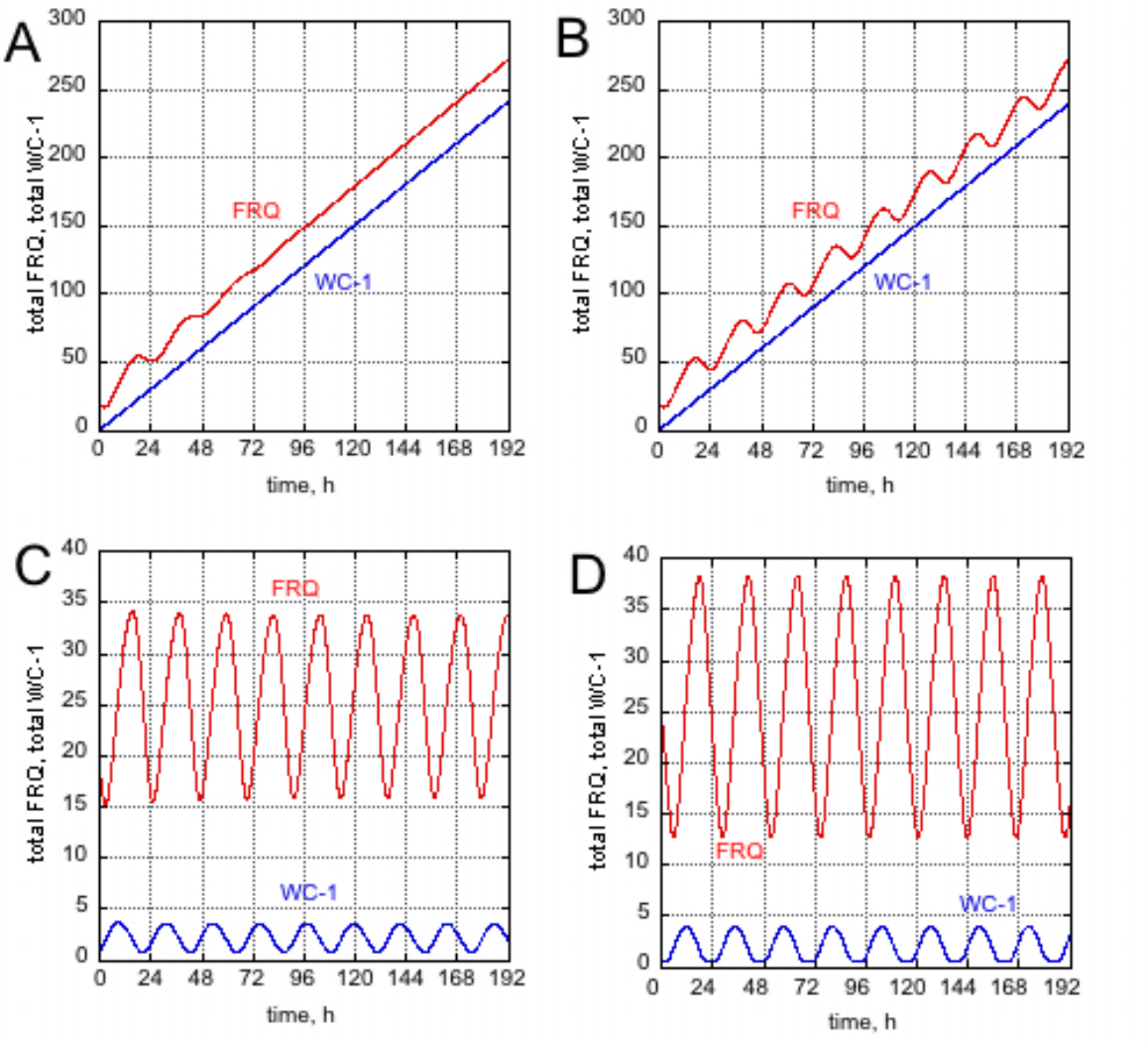

Fig. S1. FRQ-dependent clearance of nuclear WC-1 accounts for the observed *wt* phenotype. (A) Damped oscillations in the total FRQ production rate and non-oscillatory increase of total WC-1 when $k_{15}=k_{16}=k_{18}=0$ and k_{13} =50 a.u. h^{-1}. (B) Same system as in (A), but k_{13} =5 x 10^4 a.u. h^{-1}. Stable oscillations are now observed in the total FRQ production rate, while total WC-1 level still increases monotonically. (C) Sustained oscillations observed for the FRQ-dependent clearance of nuclear WC-1 using the model shown in Fig. 5A

(k_{13}=50 a.u. h^{-1}, k_{14}=1.0 h^{-1}, k_{15}=0 h^{-1}, k_{16}=100 h^{-1}, k_{17}=100 h^{-1}, and k_{18} =5 h^{-1}. (D) Sustained oscillations observed for the FRQ-dependent clearance of nuclear WC-1 for the model shown in Fig. 5B with same rate constant values for k_{13}, k_{14}, k_{15}, k_{16}, k_{17}, and k_{18} as for panel (C).

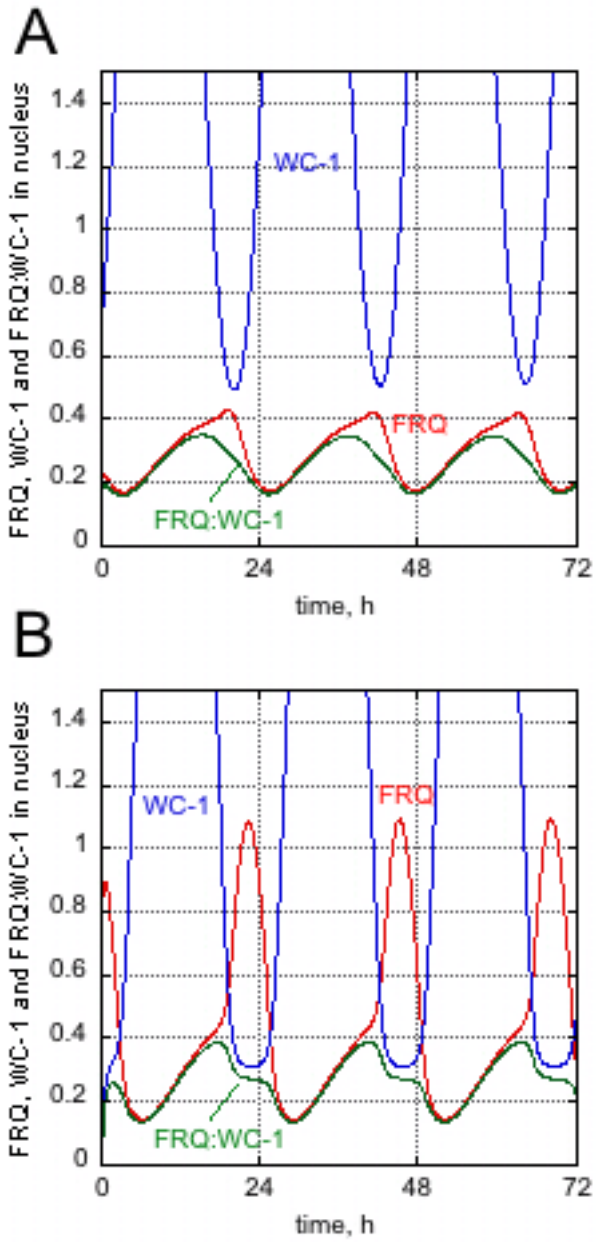

Fig. S2. Nuclear oscillation profiles for WC-1, FRQ and the FRQ:WC-1 complex. (A) Oscillations observed for the model described in Fig. 5A. For rate constant values see Table 1 and the legend for Fig. S1C. (B) Oscillations observed for the model described in Fig. 5B. For rate constant values see Table 1 and the legend for Fig. S1D.

Table 1. Rate constant values (*frq*$^{+}$ representation)

Rate constant	Value (h^{-1} or a.u. h^{-1})
k_1	1.8
k_2	1.8
k_3	0.05
$^{*}k_4$	0.23 (Ruoff et al. 1999)
$^{*}k_5$	0.27 (Ruoff et al. 2005)
k_6	0.07
k_7	0.16
k_8	0.8
k_9	40.0
	0.1 (Yu et al. 2007)

$^{*}k_{10}$	
k_{11}	0.05
k_{12}	0.02
k_{13}	5×10^{1} - 5×10^{4}
k_{14}	1.0
k_{15}	0.0
k_{16}	0.0 or 1×10^{2}
k_{17}	1×10^{2}
k_{18}	5.0
K	1.25
K_2	1.0

References

Cheng, P., Yang, Y., and Liu, Y. 2001. Interlocked feedback loops contribute to the robustness of the *Neurospora* circadian clock. *Proc Natl Acad Sci U S A* **98**(13): 7408-7413.

Denault, D.L., Loros, J.J., and Dunlap, J.C. 2001. WC-2 mediates WC-1-FRQ interaction within the PAS protein-linked circadian feedback loop of *Neurospora*. *EMBO J* **20**(1-2): 109-117.

Ermentrout, B. 2002. *Simulating, Analyzing, and Animating Dynamical Systems*. Siam, Philadelphia.

Froehlich, A.C., Liu, Y., Loros, J.J., and Dunlap, J.C. 2002. White Collar-1, a circadian blue light photoreceptor, binding to the *frequency* promoter. *Science* **297**: 815-819.

Froehlich, A.C., Loros, J.J., and Dunlap, J.C. 2003. Rhythmic binding of a WHITE COLLAR-containing complex to the *frequency* promoter is inhibited by FREQUENCY. *Proc Natl Acad Sci U S A* **100**(10): 5914-5919.

Hong, C.I., Jolma, I.W., Loros, J.J., Dunlap, J.C., and Ruoff, P. 2008. Simulating dark expressions and interactions of *frq* and *wc-1* in the *Neurospora* circadian clock. *Biophys J* **94**(4): 1221-1232.

Lee, K., Loros, J.J., and Dunlap, J.C. 2000. Interconnected feedback loops in the *Neurospora* circadian system. *Science* **289**(5476): 107-110.

Radhakrishnan, K. and Hindmarsh, A.C. 1993. Description and Use of LSODE, the Livermore Solver for Ordinary Differential Equations. In. National Aeronautics

and Space Administration, Lewis Research Center, Cleveland, OH 44135-3191.

Ruoff, P., Loros, J.J., and Dunlap, J.C. 2005. The relationship between FRQ-protein stability and temperature compensation in the *Neurospora* circadian clock. *Proc Natl Acad Sci U S A* **102**(49): 17681-17686.

Ruoff, P., Vinsjevik, M., Monnerjahn, C., and Rensing, L. 1999. The Goodwin oscillator: on the importance of degradation reactions in the circadian clock. *J Biol Rhythms* **14**(6): 469-479.

Schafmeier, T., Haase, A., Kaldi, K., Scholz, J., Fuchs, M., and Brunner, M. 2005. Transcriptional feedback of *Neurospora* circadian clock gene by phosphorylation-dependent inactivation of its transcription factor. *Cell* **122**(2): 235-246.

Schafmeier, T., Kaldi, K., Diernfellner, A., Mohr, C., and Brunner, M. 2006. Phosphorylation-dependent maturation of *Neurospora* circadian clock protein from a nuclear repressor toward a cytoplasmic activator. *Genes Dev* **20**(3): 297-306.

Yu, Y., Dong, W., Altimus, C., Tang, X., Griffith, J., Morello, M., Dudek, L., Arnold, J., and Schuttler, H.B. 2007. A genetic network for the clock of *Neurospora* crassa. *Proc Natl Acad Sci U S A* **104**(8): 2809-2814.